

# The distribution of mean and fluctuating magnetic fields in the multi-phase ISM

C. C. Evirgen<sup>1\*</sup>, F. A. Gent<sup>2</sup>, A. Shukurov<sup>1</sup>, A. Fletcher<sup>1</sup> and P. Bushby<sup>1</sup>.

<sup>1</sup>*School of Mathematics and Statistics, Newcastle University, Newcastle upon Tyne, UK, NE1 7RU*

<sup>2</sup>*ReSoLVE Centre of Excellence, Department of Computer Science, Aalto University, PO Box 15400, FI-00076 Aalto, Finland*

Accepted -. Received -; in original form -

## ABSTRACT

We explore the effects of the multi-phase structure of the interstellar medium (ISM) on galactic magnetic fields. Basing our analysis on compressible magnetohydrodynamic (MHD) simulations of supernova-driven turbulence in the ISM, we investigate the properties of both the mean and fluctuating components of the magnetic field. We find that the mean magnetic field preferentially resides in the warm phase and is generally absent from the hot phase. The fluctuating magnetic field does not show such pronounced sensitivity to the multi-phase structure.

**Key words:** dynamo – MHD – turbulence – galaxies: ISM – ISM: magnetic fields – ISM: kinematics and dynamics

## 1 INTRODUCTION

The interstellar medium (ISM) has a complex, multi-phase structure. However, very little is known about the influence that this structure has upon galactic magnetic fields. This is partly due to limitations in the observational techniques, but it should also be emphasised that galactic dynamo theory has been developed without any explicit reference to the multi-phase structure of the ISM (Beck et al. 1996; Shukurov 2007). Further theoretical progress is needed to aid the interpretation of observations.

Two types of dynamo operate in a typical spiral galaxy. The mean-field (large-scale) dynamo produces a magnetic field that is ordered on a scale larger than the turbulent scale,  $l_0 \simeq 50\text{--}100$  pc. This process relies on the differential rotation of galactic gaseous discs as well as helical turbulence in the ISM. The e-folding time of the large-scale magnetic field,  $T_{\text{MFD}}$ , is comparable to the turbulent magnetic diffusion time across the ionised gas layer, which is of the order of  $2.5 \times 10^8$  yr near the Sun. The other key dynamo mechanism is the fluctuation (small-scale) dynamo, in which local turbulent motions (which may, or may not, be helical) produce a disordered magnetic field that is structured on the scale of the flow (e.g. Zeldovich et al. 1990; Brandenburg & Subramanian 2005). The time scale at which these small-scale magnetic fields are amplified is of the order of the eddy turnover time of the turbulent flow,  $T_{\text{FD}} \simeq l_0/v_0$  ( $\simeq 10^7$  yr in the warm phase near the Sun, assuming that the scale

and speed of interstellar turbulence are  $l_0 = 100$  pc and  $v_0 = 10$  km s<sup>-1</sup>, respectively). Both types of dynamo mechanism amplify magnetic fields up to a strength of the order of a few microgauss, which corresponds to energy equipartition with the turbulence,  $B_0 \simeq (4\pi\rho v_0^2)^{1/2}$ , where  $\rho$  is the gas density.

Since the fractional volume occupied by the cold and molecular gas in the ISM is negligible, it is likely that only the warm and hot phases affect significantly dynamo action at the galactic scale. Therefore, here we focus on magnetic fields in the warm and hot diffuse gas phases. The spatial scale of the mean magnetic field, of the order of 1 kpc or more, is comparable to or exceeds the typical size of the hot regions in the ISM. Furthermore it is replenished by the dynamo at a time scale longer than the residence time of a parcel of hot gas within the gas layer,  $h/V_z \simeq 5 \times 10^6$  yr, where  $h \simeq 500$  pc is the scale height of the warm, partially ionised gas layer and  $V_z \simeq 100$  km s<sup>-1</sup> is the vertical speed of the hot gas at the base of a galactic fountain or wind. Therefore, it seems plausible that the large-scale magnetic field should be mainly produced in the warm interstellar gas that remains in an average hydrostatic equilibrium within a relatively thin layer (Shukurov 2007). It is also important to note that, given the large volume fraction occupied by the warm phase, it is likely to form, on average, a simply connected (percolating) volume in which the mean field can reside. On the other hand, the time scale of the mean-field dynamo is so much longer than the residence time of the hot gas in the warm layer that the dynamo might be controlled by ISM parameters averaged over time scales comparable to  $T_{\text{MFD}}$ ; then the mean magnetic field would permeate both the warm and hot phases. Thus, order of magnitude esti-

\* E-mails: c.c.evirgen@newcastle.ac.uk; frederick.gent@aalto.fi; anvar.shukurov@newcastle.ac.uk; andrew.fletcher@newcastle.ac.uk; paul.bushby@newcastle.ac.uk

mates alone do not provide us with sufficient information to determine which phase of the ISM maintains the large-scale magnetic field.

The time scale of the fluctuation dynamo  $T_{\text{FD}}$  also exceeds the residence time of the hot gas in the warm layer, but not by a wide margin. It is therefore plausible that the fluctuation dynamo is able to amplify the random magnetic field in the hot gas to the level of equipartition with the local turbulence only at a certain height above the galactic midplane, while the magnetic field strength in the hot gas near the midplane is significantly below equipartition as it is produced from the field of the warm phase via expansion.

The structure of this Letter is as follows. In Section 2 we briefly describe the numerical simulations which are the source of our data. The method we use to define the magnetic field lines of the mean and fluctuating magnetic field components is covered in Section 3. In Section 4 we investigate how the mean and fluctuating magnetic fields are connected to the different phases of the ISM. The main conclusions are summarised in Section 5.

## 2 SIMULATIONS OF THE MULTI-PHASE ISM

It is now possible to carry out magnetohydrodynamic (MHD) simulations of the ISM, including most of the relevant physical processes (e.g. Korpi et al. 1999a,b; de Avillez & Breitschwerdt 2005; Mac Low et al. 2005; Gressel et al. 2008; Piontek et al. 2009; Hill et al. 2012; Bendre et al. 2015; Henley et al. 2015). Our results use the simulations of supernova-driven turbulence in the multiphase ISM of Gent et al. (2013b) and Gent et al. (2013a), subsequently referred to as Paper I and Paper II, respectively. The crucial point about these simulations is that the magnetic field has not been imposed, but evolves dynamically under realistic physical conditions, including the dynamo action (see also Gressel et al. 2008; Bendre et al. 2015). The numerical model solves the non-ideal MHD equations (described in detail in Gent 2012, Section 3), in a local box of  $1 \times 1 \text{ kpc}^2$  horizontally and  $-1 < z < 1 \text{ kpc}$  vertically in size, with the galactic midplane at  $z = 0$ . Gravity due to stellar mass and the dark halo follows Kuijken & Gilmore (1989). All models are subject to radiative cooling (Sarazin & White 1987; Wolfire et al. 1995), photoelectric heating (Wolfire et al. 1995) and other transport processes, which are necessary to support the multiphase structure. Local estimates for the differential rotation, supernova rate and distribution, and column density are used (see Ferrière 2001). A nanogauss seed magnetic field is amplified by dynamo action until it saturates with a typical magnetic field strength of a few microgauss.

We follow Gent (2012) in defining the three phases of the ISM in terms of specific entropy  $s$ , expressed as

$$s = c_V [\ln(T/T_0) - (\gamma - 1) \ln(\rho/\rho_0)], \quad (1)$$

where  $\rho$  (base unit,  $\rho_0 = 1 \text{ g cm}^{-3}$ ) and  $T$  (base unit,  $T_0 = 1 \text{ K}$ ) denote density and temperature, respectively,  $c_V$  is the specific heat capacity at constant volume, and the adiabatic index is  $\gamma = 5/3$ . Using Eq. (1) and in units of  $10^8 \text{ erg g}^{-1} \text{ K}^{-1}$ , the cold phase is defined as  $s < 4.4$ , the warm phase as  $4.4 < s < 23.2$ , and the hot phase as  $s > 23.2$ . The phases of the ISM can also be defined according to temperature and density. The phase definitions are listed in Table 1

**Table 1.** Parameters of the ISM phases: specific entropy  $s$  [ $10^8 \text{ erg g}^{-1} \text{ K}^{-1}$ ], defined in Eq. (1), temperature  $T$  [K] and density  $\rho$  [ $\text{g cm}^{-3}$ ]. The phases are in pressure equilibrium, with total pressure log-normally distributed about  $10^{-12.5} \text{ dyn cm}^{-2}$  (Gent 2012, Figure 5.11d).

ISM phase	Cold	Warm	Hot
$s$	$s < 4.4$	$4.4 < s < 23.2$	$s > 23.2$
$T$	$T < 500$	$500 < T < 5 \cdot 10^5$	$T > 5 \cdot 10^5$
$\rho$	$\rho > 10^{-24}$	$10^{-26} < \rho < 10^{-24}$	$\rho < 10^{-26}$

together with the typical temperature and density within these entropy ranges.

We consider volume and time averages of physical variables from 23 snapshots from a nonlinear MHD model that has twice the galactic rotation rate of the solar neighbourhood. Integrating MHD models to attain dynamo saturation is computationally expensive (even the most efficient dynamo from Paper II took over 1 Gyr to reach saturation). Our choice of rotation rate is a pragmatic one, designed to optimise the efficiency of the dynamo. We will consider models with lower rotation rates in future work. To illustrate the difference that a magnetic field makes to the phase-structure of the ISM we also consider snapshots taken from the kinematic phase of the dynamo, during which the field is too weak to influence its surroundings.

## 3 THE MEAN AND FLUCTUATING MAGNETIC FIELDS

The decomposition of the magnetic field into mean and fluctuating (random) parts follows the method described in Paper II. Volume averaging with a Gaussian kernel  $G_l(\mathbf{x} - \mathbf{x}')$  of a scale  $l$  is used to split the magnetic field  $\mathbf{B}$  into mean,  $\mathbf{B}_l$ , and random,  $\mathbf{b}_l$ , parts:

$$\mathbf{B} = \mathbf{B}_l + \mathbf{b}_l, \quad \mathbf{B}_l = \langle \mathbf{B} \rangle_l, \quad (2)$$

where angular brackets denote an average calculated as

$$\langle \mathbf{B} \rangle_l(\mathbf{x}) = \int_V \mathbf{B}(\mathbf{x}') G_l(\mathbf{x} - \mathbf{x}') d^3 \mathbf{x}', \quad (3)$$

$$G_l(\mathbf{x}) = (2\pi l^2)^{-3/2} \exp[-\mathbf{x}^2/(2l^2)],$$

where  $l \approx 50 \text{ pc}$  is half the integral scale of the turbulent motions in the numerical model (see Paper II for further details). Preliminary analysis does not show significant sensitivity of the mean or random field to variations in  $l$  within the range  $30 < l < 100 \text{ pc}$ .

Given a magnetic field,  $\mathbf{B}(\mathbf{x})$ , in Cartesian coordinates, its integral (field) lines are described by

$$\frac{dx}{B_x} = \frac{dy}{B_y} = \frac{dz}{B_z} = \frac{dr}{|\mathbf{B}|}, \quad (4)$$

where  $dr$  is the line element measured along the line. We obtain the integral lines for both the mean and fluctuating magnetic fields by integrating these equations, using a fourth-order Runge-Kutta scheme, applying linear interpolation between the grid points.

Our aim is to determine whether the mean and fluctuating magnetic fields are predominantly located in specific phases of the ISM. However, it is not straightforward to find

a robust quantitative measure for this. The spatial distribution of magnetic energy density is biased towards the cold, dense gas that occupies a negligible fraction of the volume. We suggest a different approach, based on a comparison of the statistical properties of specific entropy along field lines with those in the entire volume. If a magnetic field does not prefer to reside in any particular phase, the probability density function (PDF) of specific entropy sampled along the field lines should be the same as the volume PDF. Conversely, if a magnetic field is sensitive to the multi-phase structure, the difference between the field-line and volume PDFs of specific entropy will highlight the entropy interval(s), and thus the phase(s) where differences arise.

#### 4 MAGNETIC FIELDS IN THE MULTI-PHASE STRUCTURE

Figure 1(a) compares  $\mathcal{P}_V(s)$ , the volume-sampled specific entropy PDF, with  $\mathcal{P}_B(s)$ , the corresponding PDF sampled along the mean magnetic field lines. These plots indicate that the mean magnetic field tends to favour the low entropy zone of the warm phase; the peak of  $\mathcal{P}_B(s)$  is located at  $s = 12$  (the specific entropy is expressed here, and elsewhere in the text, in units of  $10^8 \text{ erg g}^{-1} \text{ K}^{-1}$ ), whereas the corresponding peak in  $\mathcal{P}_V(s)$  is located at  $s = 15$ . For  $18 \lesssim s < 23$ ,  $\mathcal{P}_B(s)$  is systematically lower than  $\mathcal{P}_V(s)$ . Furthermore, for entropy values in the range  $s > 23$ ,  $\mathcal{P}_B(s)$  is significantly lower than  $\mathcal{P}_V(s)$ , which suggests that the mean field avoids the hot gas. Figure 1(b) shows a comparison between  $\mathcal{P}_V(s)$  and  $\mathcal{P}_b(s)$ , which is the PDF of specific entropy along the fluctuating (random) magnetic field. The differences between these curves are less dramatic than those shown in Figure 1(a). Whilst  $\mathcal{P}_b(s)$  systematically has a higher probability density than  $\mathcal{P}_V(s)$  for  $s < 15$ , the difference is clearly smaller than for  $\mathcal{P}_B(s)$ . The random field component is suppressed to some extent in the hot phase, but this is less pronounced than it is for the mean magnetic field.

Figure 2 uses a single snapshot in the nonlinear regime to give an alternative view of these results. In panel (a), there is a large column (chimney) of hot, high-entropy gas spanning the domain horizontally and vertically, from which mean magnetic field lines appear to be absent. This is consistent with the PDFs shown in Figure 1, further reinforcing the idea that the mean magnetic field is sensitive to the multi-phase structure. Panel (b) shows that the mean magnetic field, where it is found, tends to be approximately aligned with the azimuthal ( $y$ ) direction (as it is affected by the velocity shear). Panels (c) and (d) show the random (fluctuating) magnetic field in the same snapshot. As expected, the field lines do not appear to have a preferred direction. In addition, the random magnetic field lines do not appear to avoid the column of hot gas in the same way as the mean field. Thus, the random magnetic field appears to be less sensitive to the multi-phase structure.

It is plausible that the relative reduction in the strength of the mean magnetic field in the hot gas is explained by the rapid expansion of hot gas bubbles. Furthermore, the hot gas is removed from the galactic disc over a time scale significantly shorter than the mean-field dynamo time scale. Figure 3 shows that the mean and random magnetic fields

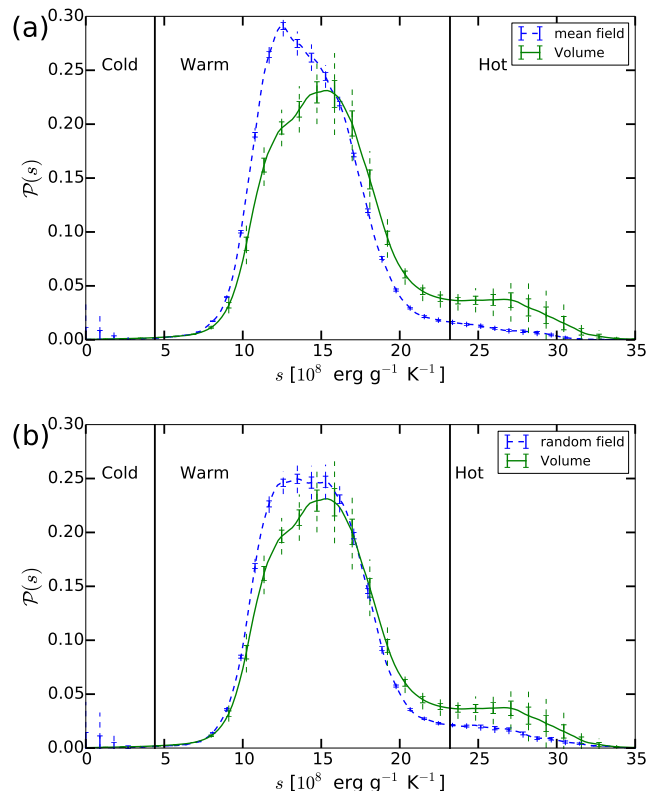


**Figure 1.** The probability density functions (PDFs) of specific entropy in the whole computational volume (solid) and sampled along the integral lines (dashed) of the (a) mean and (b) random magnetic fields. Vertical lines show the boundaries between the cold, warm and hot ISM phases.

reach their maximum amplitude away from the midplane, just outside the layer  $|z| \lesssim 0.2 \text{ kpc}$  where most of the supernovae are located. We note that the random magnetic field strength remains of order  $1 \mu\text{G}$  for  $|z| < 0.2 \text{ kpc}$ , whilst the mean magnetic field increases from  $1.7 \mu\text{G}$  at the midplane to  $2.8 \mu\text{G}$  at  $|z| = 0.3 \text{ kpc}$ . The mean field strength at the midplane is remarkably consistent with the observed estimate of [Rand & Kulkarni \(1989\)](#). However, we note that the strength of the random magnetic field in our simulations is significantly lower than the  $5 \mu\text{G}$  observed in the solar vicinity of the Milky Way ([Beck et al. 1996](#); [Haverkorn 2015](#)). Whilst we do not believe that this discrepancy affects our main conclusions regarding the distribution of the field across the ISM phases, the reason for this difference is not obvious. It may indicate that the fluctuation dynamo (which directly generates small scale field) is less efficient than it should be, so that the simulated random field is due primarily to the tangling of mean magnetic field lines by the turbulent velocity field. Another possibility is the (implicit) use of longer averaging scales in the interpretation of the observations. Our domain size of  $1 \text{ kpc}$  limits the smoothing scale that we can apply. However, these possibilities are speculative and more work is required to properly understand the relatively weak random field in the simulations.

Figure 3 also shows the random velocity  $|\tilde{\mathbf{u}}|$  (defined in the rotating frame with the mean vertical flow deducted)

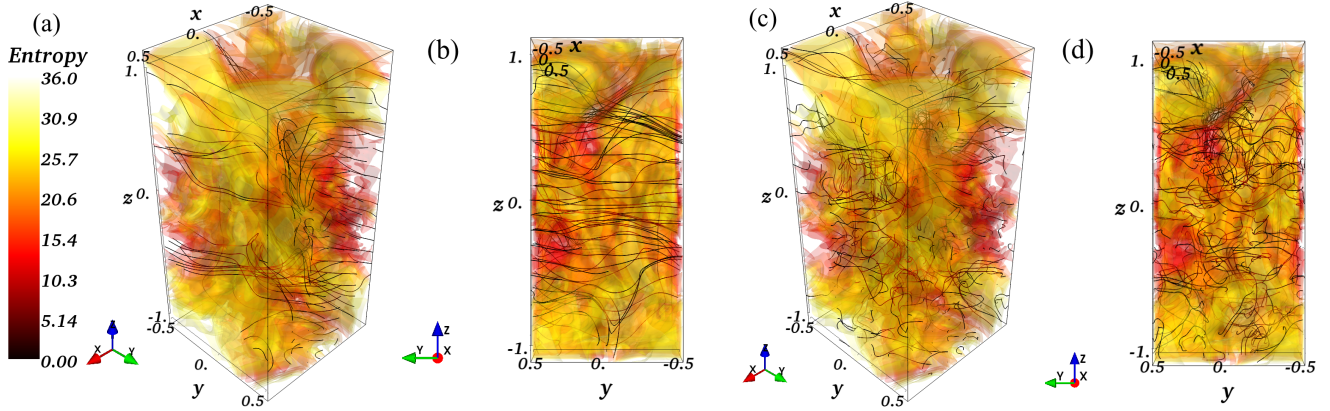


**Figure 2.** 3D rendering of magnetic field lines (black) in the simulated ISM, with the specific entropy of the gas in the background (colour, in the units of  $10^8 \text{ erg g}^{-1} \text{ K}^{-1}$ ). Panels (a) and (b) show the mean-field lines and panels (c) and (d) the random field lines. Panels (a) and (c) give an isometric view, and panels (b) and (d) show a view through the  $(y, z)$  plane. Cartesian coordinates  $(x, y, z)$  locally correspond to the cylindrical polar coordinates  $(r, \phi, z)$  with the  $z$ -axis aligned with the angular velocity of galactic rotation.

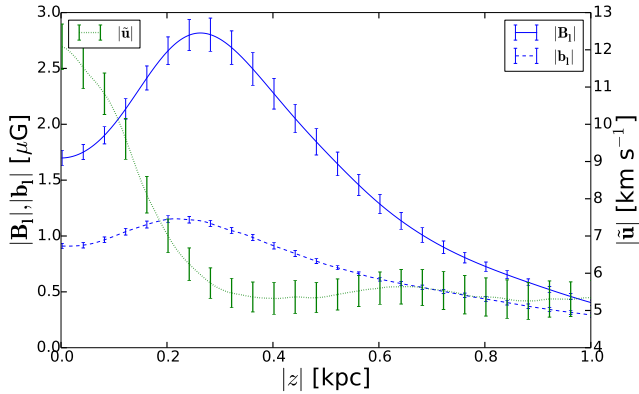


**Figure 3.** Horizontal averages of mean magnetic field strength  $|B_l|$  (solid lines), random magnetic field strength  $|b_l|$  (dashed lines) and random velocity  $|\bar{u}|$  (dotted lines), shown as functions of distance from the midplane.

for which there is a local maximum at the midplane, where the supernovae dominate the dynamics. Away from the midplane, the random velocity decreases rapidly reaching a minimum value at approximately  $|z| \sim 0.4$  kpc, where the mean magnetic field is strong. At larger values of  $|z|$ , the amplitudes of the mean and fluctuating components of the magnetic field both decrease with increasing distance away from the midplane. In this region, the mean magnetic field strength decreases from its maximum,  $2.8 \mu\text{G}$ , to  $0.4 \mu\text{G}$ . The decrease in random magnetic field strength is more modest ( $1$  to  $0.3 \mu\text{G}$ ). The variation of the magnetic field with  $|z|$  suggests that the most efficient dynamo action is confined primarily to regions within a few hundred parsecs of the midplane.

Figure 4 displays the PDFs of specific entropy in the whole computational domain during both the early kinematic and nonlinear (saturated) dynamo stages. There is a difference in the distribution of entropy between the ISM with a dynamically-insignificant (i.e. kinematic) magnetic field and the ISM with a dynamo-generated magnetic field that has saturated. Whilst the modal probabilities of the

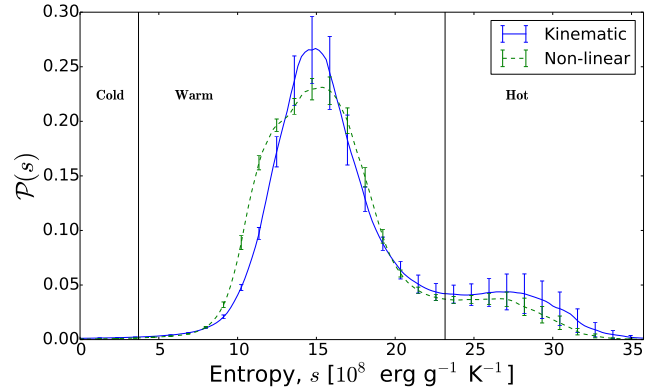


**Figure 4.** Probability density of specific entropy in the computational domain for the kinematic (solid) and nonlinear (dashed) state of the dynamo. Vertical lines show the boundaries between the cold and warm ISM phases and the warm and hot phases.

warm and hot phase are similar, the shape of the distribution is different. In the case of a saturated dynamo, the PDF is wider in the warm phase, and has a region of higher probability density in  $10 < s < 12$ . In addition, saturation of the dynamo leads to a consistent reduction of probability density for the higher entropy gas with  $s > 20$ . Even though there is clear evidence for the existence of a warm and hot phase the entropy distributions within the phases change as the magnetic field grows.

Further insight into the mean-field dynamo mechanism can be gained by examining the electromotive force (EMF). Denoted by  $\mathcal{E}$ , the EMF can be expressed as a sum of its mean,  $\mathcal{E}_l$ , and fluctuating,  $\mathcal{E}'$ , parts. These are calculated as follows:

$$\mathcal{E} = \mathbf{u} \times \mathbf{B}, \quad \mathcal{E}_l = \langle \mathbf{u} \times \mathbf{B} \rangle_l, \quad \mathcal{E}' = \mathcal{E} - \mathcal{E}_l,$$

where  $\mathbf{u}$  denotes the total velocity field in the rotating frame. Summary statistics for the mean and fluctuating EMF are given in Table 2. These values indicate that the mean EMF in the warm phase is approximately twice as strong as it is in the hot phase, which supports the idea that dynamo

**Table 2.** Averages of the mean and fluctuating EMF strength over the volumes  $\mathcal{V}$  occupied by the warm or hot phases.  $\mathcal{E}_\ell = \langle |\mathcal{E}_\ell| \rangle_{\mathcal{V}}$  and  $\mathcal{E}' = \langle |\mathcal{E}'| \rangle_{\mathcal{V}}$ , with standard deviation denoted by  $\sigma_\ell$  and  $\sigma'$ , respectively [ $\text{G km s}^{-1}$ ].

	$\mathcal{E}_\ell$	$\sigma_\ell$	$\mathcal{E}'$	$\sigma'$
Warm	1.12	0.91	1.01	1.14
Hot	0.65	0.72	1.03	1.91

action in the mean field is strongest in the warm phase. The warm and hot phases have similar values for the fluctuating part of the EMF.

## 5 CONCLUSIONS AND DISCUSSION

We have shown that the mean magnetic field is sensitive to the multiphase structure of the ISM. Our PDF analysis indicates that it resides preferentially in the lower entropy region of the warm phase, particularly in the layer  $0.2 < |z| < 0.4$  kpc, avoiding regions of hotter gas. Given the presence of the velocity shear, it is unsurprising that this mean field tends to be aligned with the  $y$ -coordinate (i.e. the azimuthal direction) in our model. The random magnetic field appears to be less strongly influenced by the multiphase structure. As functions of distance from the midplane ( $z = 0$ ), the mean and random magnetic field strengths peak at  $|z| = 300\text{pc}$  and  $|z| = 200\text{pc}$ , respectively.

The marginal preference of the fluctuating field for low entropy regions of the warm phase is likely due to generation of the random field by tangling of the mean field produced by the large-scale dynamo. Small-scale dynamo action may not be fully resolved with the grid resolution of 4 pc in these simulations, and so may be less efficient than it should be, but this interpretation is speculative. Separating the two different mechanisms, by which the random field can be produced is subtle and difficult; we shall return to this problem in subsequent work that examines how galactic dynamos saturate in the multi-phase ISM.

There is an increasing fractional volume of gas within the warm phase, as the mean magnetic field grows and saturates. Whilst it was expected that the magnetic field preferentially resides in the warm phase, this result suggests that dynamo action actively changes the volume entropy distribution, and thus the multi-phase structure of the ISM. This raises a significant question: does the magnetic field preferentially reside in the warm phase, or does it adapt the multi-phase structure, in order to create a hospitable environment for dynamo action? In other words, how does the multi-phase structure change as the ISM becomes magnetised? We will discuss these questions, which can have important consequences for galactic evolution, in future work.

## ACKNOWLEDGEMENTS

AS is grateful to Carl Heiles, Richard Crutcher and Thomas Troland for useful discussions of magnetic fields in the hot interstellar gas. FAG acknowledges financial support of the Grand Challenge project SNDYN, CSC-IT Center for Science Ltd. (Finland) and the Academy of Finland

Project 272157. AS, AF and PB were supported by the Leverhulme Trust Grant RPG-2014-427 and STFC Grant ST/N000900/1 (Project 2). CCE was supported by the RAS and Nuffield Foundation with an RAS Undergraduate Bursary, entitled ‘‘Magnetic Fields and Turbulence in the Multi-phase Interstellar Medium’’. We would also like to thank the referee for useful comments and suggestions.

## REFERENCES

- de Avillez M. A., Breitschwerdt D., 2005, *A&A*, **436**, 585
- Beck R., Brandenburg A., Moss D., Shukurov A., Sokoloff D., 1996, *ARA&A*, **34**, 155
- Bendre A., Gressel O., Elstner D., 2015, *Astron. Nachr.*, **336**, 991
- Brandenburg A., Subramanian K., 2005, *Phys. Rep.*, **417**, 1
- Ferrière K. M., 2001, *Rev. Mod. Phys.*, **73**, 1031
- Gent F. A., 2012, PhD thesis, Newcastle University School of Mathematics and Statistics, <http://hdl.handle.net/10443/1755>
- Gent F. A., Shukurov A., Sarson G. R., Fletcher A., Mantere M. J., 2013a, *MNRAS*, **430**, L40
- Gent F. A., Shukurov A., Fletcher A., Sarson G. R., Mantere M. J., 2013b, *MNRAS*, **432**, 1396
- Gressel O., Elstner D., Ziegler U., Rüdiger G., 2008, *A&A*, **486**, L35
- Haverkorn M., 2015, in Lazarian A., de Gouveia Dal Pino E. M., Melioli C., eds, *Magnetic Fields in Diffuse Media*. Springer, Berlin, p. 483
- Henley D. B., Shelton R. L., Kwak K., Hill A. S., Mac Low M.-M., 2015, *ApJ*, **800**, 102
- Hill A. S., Joung M. R., Mac Low M.-M., Benjamin R. A., Haffner L. M., Klingenberg C., Waagan K., 2012, *ApJ*, **750**, 104
- Korpi M. J., Brandenburg A., Shukurov A., Tuominen I., 1999a, *A&A*, **350**, 230
- Korpi M. J., Brandenburg A., Shukurov A., Tuominen I., Nordlund Å., 1999b, *ApJ*, **514**, L99
- Kuijken K., Gilmore G., 1989, *MNRAS*, **239**, 605
- Mac Low M.-M., Balsara D. L., Kim J., Avillez M. A. D., 2005, *ApJ*, **626**, 864
- Piontek R. A., Gressel O., Ziegler U., 2009, *A&A*, **499**, 633
- Rand R. J., Kulkarni S. R., 1989, *ApJ*, **343**, 760
- Sarazin C. L., White R. E., 1987, *ApJ*, **320**, 32
- Shukurov A., 2007, in Dormy E., Soward A. M., eds, *Mathematical Aspects of Natural Dynamos*. Chapman & Hall/CRC, pp 313–359
- Wolfire M. G., Hollenbach D., McKee C. F., Tielens A. G. G. M., Bakes E. L. O., 1995, *ApJ*, **443**, 152
- Zeldovich Ya. B., Ruzmaikin A. A., Sokoloff D. D., 1990, *The Almighty Chance*. World Scientific, Singapore